Physicochemical Nature of Perfluoroalkyl Compounds Induced by Fluorine

AUTHOR(S):

Hasegawa, Takeshi

Physicochemical Nature of Perfluoroalkyl Compounds Induced by Fluorine

Takeshi Hasegawa*[a]

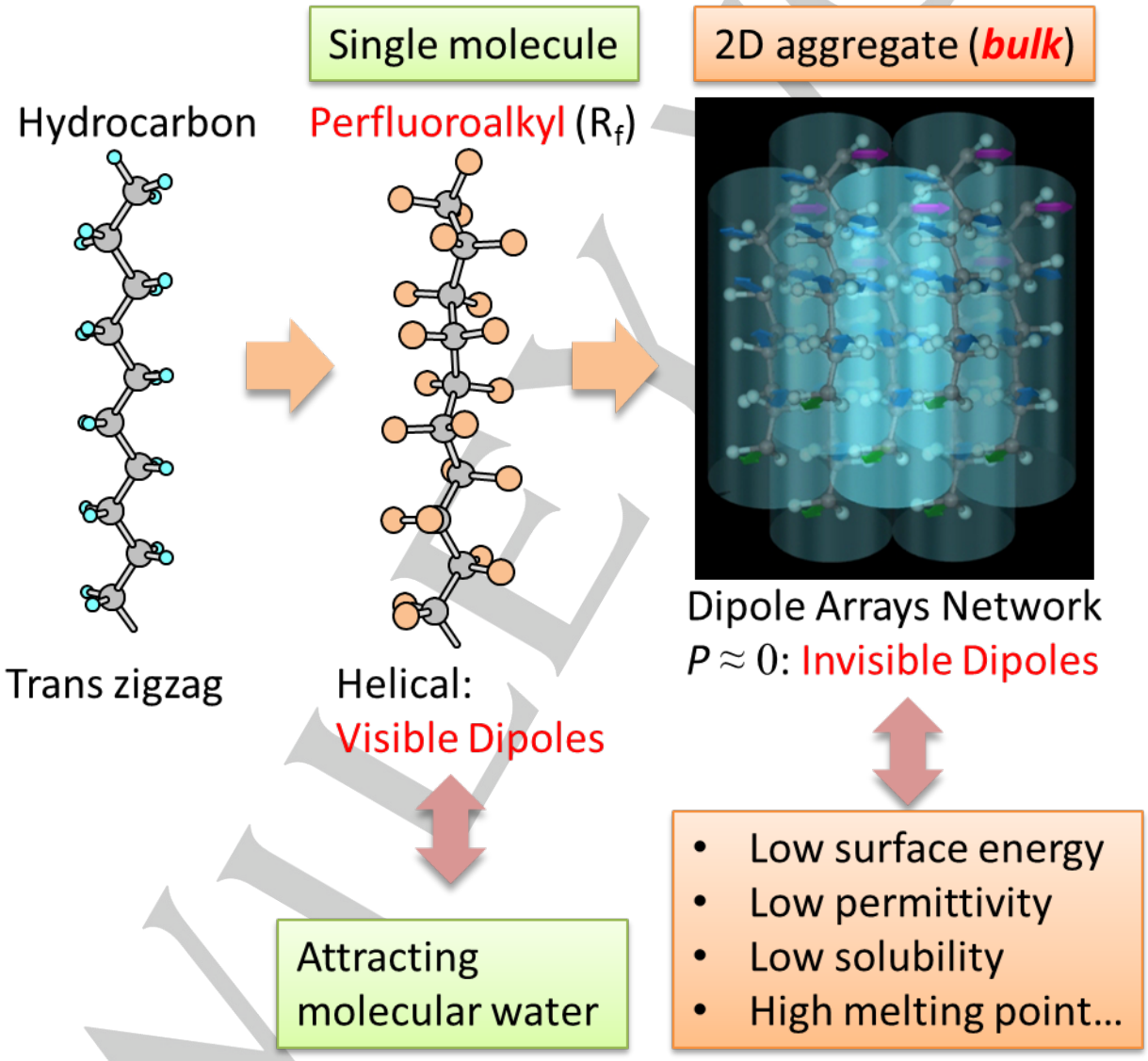

[a] Professor, T. Hasegawa
Institute for Chemical Research
Kyoto University
Gokasho, Uji, Kyoto-fu 611-0011, Japan
E-mail: htakeshi@scl.kyoto-u.ac.jp

Abstract: Perfluoroalkyl (R_f) compounds have unique characters represented by a significantly high hydrophobic property, which often makes us consider that R_f groups should be interacted with each other via the 'hydrophobic interaction' as found for a normal hydrocarbon. Due to a similar intuitive and simplistic speculation, the R_f-specific material properties have long been enveloped in darkness for comprehensive understanding, which should lucidly be discussed within a framework of physical chemistry. Here, we show studies on the stratified dipole arrays (SDA) theory, which readily explains the R_f-specific material characters in a comprehensive manner based on only a few fundamental physical parameters of fluorine. The SDA theory encompasses some conventional theories that account for only a part of material properties. In addition, we show that the concept of vibrational spectroscopy of R_f compounds should also be revised, since the mass of fluorine is larger than that of carbon, which is opposite to the hydrocarbon case. In this manner, chemistry of R_f compounds needs another fully revised concept, which cannot be replaced by an extended concept of normal hydrocarbon compounds.

1. Introduction

Fluorine is a unique element, which can be a highly stable replacement of hydrogen atoms in a hydrocarbon compound.[1] A fully fluorine-substituted alkyl group is called a "perfluoroalkyl" group that is often denoted by a symbol of "R_f." R_f compounds are used in a wide range of practical applications, and PTFE (polytetrafluoroethylene or polytetrafluoroethene; known as Teflon®) is a representative, which is widely used in daily life due to the R_f-specific material properties represented by the water/oil repellency, high melting point, low electric permittivity (or low refractive index) and insoluble character for many organic solvents, which has a long history more than seventy years.

To our surprise, however, the physicochemical nature generating the useful properties has long been unclear thus far. In fact, the material design has mostly been carried out on experiences, which makes fluorochemistry only for specialists having much experience. This is indeed a vicious cycle for the comprehensive understanding of R_f compounds on the chemical structure.

One of the reasons to generate the scientifically unsound tradition should be attributed to 'ambiguous terminology' that is often conveniently used in many chemistry communities.[2] For example, "hydrophobic" is used in at least three different meanings: 1) insoluble in water, 2) soluble in oil, and 3) exhibiting a large contact angle. Although these phenomena are on totally different chemical/physical principles, they are often discussed by using a common term of "hydrophobic." This is an unfavorable habit, which makes chemists blind to the truth. In a similar manner, a term of "hydrophobic interaction" is conveniently used in place of London's "dispersion force" for considering molecular interaction. Since many R_f-containing compound exhibits a hydrophobic property, R_f groups are often considered to be interacted with each other via the "hydrophobic interaction," which results in a serious confusion that the R_f-interaction should also be driven by the "dispersion force," as found in a normal hydrocarbon.

As a matter of fact, the intrinsic molecular interaction between R_f groups is *not* driven by the dispersion force, but by the dipole-dipole interactive force (Sect. 2.1), which is a decisive point for discriminating an R_f compound from a normal hydrocarbon one.[3] In other words, the physically important nature of the R_f compounds is missed by using the term of "hydrophobic interaction." In this manner, a convenient replacement of terminology sometimes makes the discussion confusing.

An essential concept for the comprehensive understanding of material properties of R_f compounds is that the property of a 'single molecule' should strictly be discriminated from that of a 'bulk' matter. For example, the water repellency is found only on a bulk matter; whereas a single R_f molecule has a totally different property, which is described in detail later. Secondly, the spontaneously aggregation of R_f groups in a two-dimensional (2D) manner plays another crucial role. This aggregation is induced by the R_f-specific helical conformation and the dipole-dipole interaction cooperatively, which are neither found in a normal hydrocarbon system. An electrodynamic mechanism on this 2D dipole-arrays network is a key to comprehensively understand the "mysterious" properties uniquely found for R_f-containing compounds.

The intrinsic difference between a normal hydrocarbon and an R_f compound is found not only for material property, but also for vibrational spectroscopy represented by infrared (IR) and Raman spectroscopy. The symmetric CH_2 stretching vibration band of an all-trans zigzag hydrocarbon chain has already theoretically been known to appear at different positions in IR and Raman spectra at about 2851 and 2848 cm^{-1}, respectively.[4] Since the difference is minor, regardless, this non-coincidence is rarely discussed even by a spectroscopist. On the other hand, an R_f group is known to exhibit a huge non-coincidence by theoretical analysis of the vibrating chain as a coupled oscillator.[5,6] In fact, the symmetric CF_2 stretching vibration band appears at largely different positions at ca. 1150 and 720 cm^{-1} in IR and Raman spectra, respectively.[5,6] This strongly implies that an R_f group requires an intrinsically different scheme of molecular vibration from a hydrocarbon. As mentioned in Sect. 3, special care must thus be taken for some crucial points for appropriately discussing IR spectra of an R_f-containing compound. Once we have the renewed spectroscopic

[a] Professor, T. Hasegawa
Institute for Chemical Research
Kyoto University
Gokasho, Uji, Kyoto-fu 611-0011, Japan
E-mail: htakeshi@scl.kyoto-u.ac.jp

concept, however, IR spectroscopy becomes indeed a quite powerful and convenient tool for analyzing molecular structure and arrangement of R_f groups in a material.

In this review, recently established physicochemical schematics for comprehensive understanding of the nature of R_f compounds are mentioned with respect to both theoretical and experimental studies.

Professor Takeshi Hasegawa received B.S. degree from Waseda University, and M.S. and PhD from Kyoto University. He was appointed to be Assistant Professor at Kobe Pharmaceutical University in 1993 and Lecturer in 2001. After he experienced Associate Professor at CIT, Nihon University (2003), Researcher of JST PRESTO (2004), and Associate Professor at Tokyo Institute of Technology (2006), he joined ICR, Kyoto University as Full Professor in 2011. He is a Fellow of Society for Applied Spectroscopy (USA) after recognition of his original spectroscopic technique of "pMAIRS," with which members of his laboratory are engaged in study of molecular structure in a two-dimensional molecular aggregate. Fluorochemistry is one of his top interests in this science.

2. Fluorophilicity

The molecular interaction between R_f groups has long been argued on largely different attitudes. Some people believe that R_f groups are weakly interacted with each other; whereas the rest people consider that the R_f groups are fairly strongly interacted to generate a tight molecular aggregate. The bottom line of this argument is that both attitudes are correct, and it depends on the primary chemical structure as understood on the SDA theory (Sect. 2.2). The R_f-specific molecular spontaneous aggregation is conveniently called 'fluorous'[7] or 'fluorophilic' effect.[1] The chemical mechanism inducing the fluorophilic effect is a critical key to understand the material properties of R_f compounds.

2.1. Intrinsic Molecular Interactive Forces between R_f groups

Among the many R_f-specific material characters, the most fundamental one is the high melting point, which is of course not a character of a single molecule, but of a 'bulk' matter. To discuss melting point, molecular interaction must thus be discussed in a physicochemical framework.

The non-covalent molecular interaction in a condensed matter is mostly driven by the Coulomb (~250 kJ mol^{-1}), hydrogen-bonding (HB; ~25 kJ mol^{-1}), and van der Waals (~2 kJ mol^{-1}) interactions in a decreasing order.[8,9] For an organic compound having no apparent charge and no HB counterpart, the rest van der Waals forces are the driving force to make the molecules aggregated, which is famous for the condensation of heavy halogen molecules such as Br_2 (liquid) and I_2 (solid) at ambient temperature. In this section, such a compound driven by the weak van der Waals forces is discussed.

London first revealed a fundamental physical framework of van der Waals forces on quantum mechanics,[10] which are composed of three factors: the orientation, induction and dispersion forces. The first two factors had already been theorized by Keesom and Debye, respectively, on classical mechanics; whereas the last factor was first deduced by London himself. The three forces, $\bar{U}$, for intermolecular long-range forces are represented as follows.

$$\bar{U}_{\text{orientation}} = -\frac{1}{3R^6}\frac{\mu^4}{k_B T}\left(1+3\cos^2\theta\right) \quad (1)$$

$$\bar{U}_{\text{induction}} = -\frac{2}{R^6}\mu^2\alpha \quad (2)$$

$$\bar{U}_{\text{dispersion}} = -\frac{3}{4R^6}h\nu_0\alpha^2 \quad (3)$$

The negative sign means that the forces are 'attractive.' The three forces driven by R^{-6} are categorized into van der Waals forces.[8,9] Here, R is the distance between two molecules, and μ and α represent a dipole moment and a molecular (or atomic) polarizability, respectively. Eq. (1) is used for calculating the interactive force between two molecules having permanent dipole moments. Since the moment is a vector, the interaction depends on the relative orientation angle, θ, which is why this interaction is named "orientation force."[10]

The induction force is for an interaction between a molecule having a permanent dipole moment and another molecule having no permanent dipole. The charge distribution in the second molecule is changed by the dipole moment of the first one to have an induced dipole, which makes the two molecules attracted. Since the induced dipole moment, p, is induced by external electric field, E, via the *molecular* polarizability, α (Eq. (4)),[11] the induction force involves both α and μ as found in Eq. (2).[10]

$$p = \alpha E \quad (4)$$

The dispersion force discovered by London is a unique force, which is a quantum mechanics-driven force between two molecules having no permanent dipole. Of interest is that the dispersion force involves α only, and as a result, the three equations have a beautiful symmetry in terms of μ and α, which implies that the three principles are good enough to understand van der Waals forces. $h\nu_0$ in Eq. (3) is the absorption energy, which can be replaced by the first ionization energy as mentioned by London.[10] Since the London theory treats only one absorption energy, the equation cannot be employed for discussing molecular interaction "in a solvent" as pointed out by McLachlan.[12] Nonetheless, it is still powerful to reveal the intrinsic difference between the molecular interactions of hydrocarbons and those of R_f compounds.

For revealing the intrinsic driving force between two same molecules, in a similar manner of London's calculations, the interactive forces are calculated by using Eqs. (1)~(3) for two C–H fragments or two C–F ones, respectively, as presented in Table 1.[3]

Table 1. The three van der Waals forces between two C–H or C–F fragments.

	μ /D	α /x10^{-30} m^3	IE /eV	orientation /x10^{-79} Jm^3	induction /x10^{-79}Jm^3	dispersion /x10^{-79} Jm^3
C–H	0.40	0.652	10.64	0.422 (6.96%)	0.209 (3.44%)	5.43 **(89.6%)**
C–F	1.39	0.555	9.11	61.5 **(91.8%)**	2.14 (3.20%)	3.37 (5.03%)

The interactive force between two C–H fragments is found to be mostly governed by the dispersion force (89.6%) as expected for the hydrocarbon compounds. This explains the reason why van der Waals force is often solely attributed to the dispersion force. On the other hand, for two C–F fragments, the dominant force is changed to be the dipole-dipole interaction (orientation force; 91.8%). Although this is a very rough estimation, the comparison is good enough to reveal the intrinsic difference between the hydrocarbon and R_f groups. In short, R_f compounds cannot be discussed in an extended or corrected way of hydrocarbons using a concept of the dispersion force.

2.2. SDA theory on the dipole-dipole interaction

The material property of a molecular aggregate is discussed on the dipole-dipole interaction. Since a 'single' R_f group consists of C–F bonds having a large permanent dipole moment (Table 1), the envelope of a single R_f group should have an affinity to a water 'molecule' (not droplet) via the dipole-dipole interaction, which will be confirmed in Sect. 2.6. Then, the famous hydrophobic property is attributed to a molecular 'aggregate' of the R_f compound as discussed below.

Here, we have to note that an R_f group is characterized by its unique "helical" conformation about the molecular axis[13-15] as illustrated in Figure 1a, which depends on the phase diagram.[5,6,16] Normal alkyl groups are known to have a trans-zigzag conformation in a crystal,[17] which is an intrinsic difference from the R_f groups.

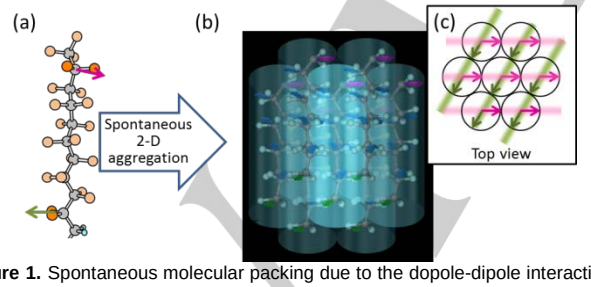

Figure 1. Spontaneous molecular packing due to the dopole-dipole interaction. (a) An R_f group with a helical conformation has dipole moments with different directions on a carbon. (b) The molecules are interacted with each other by forming (c) the dipole arrays (pink and green "lines"), which is simplified in the top view. The R_f length is interpreted as the twisting angle between the top and bottom dipoles of the CF_2 groups represented by the pink and green arrows, respectively.

This difference of the conformations is straightforwardly reflected by the melting point depending on the chain length. As found in Figure 2, normal alkanes exhibit the even-odd effect due to the trans-zigzag conformation[18-20]; whereas the R_f alkanes have a largely different trend: an apparent jump appears at the length of $(CF_2)_7$, and the melting point becomes much higher than that of normal alkanes.[21] The critical length of $(CF_2)_7$ has long been known as the magic number, and many bulk properties are influenced by this length. For example, a polyfluoroacrylate having R_f group-containing side chains is known to lose the hydrophobicity for the R_f length of $(CF_2)_6$ or shorter [22,23].

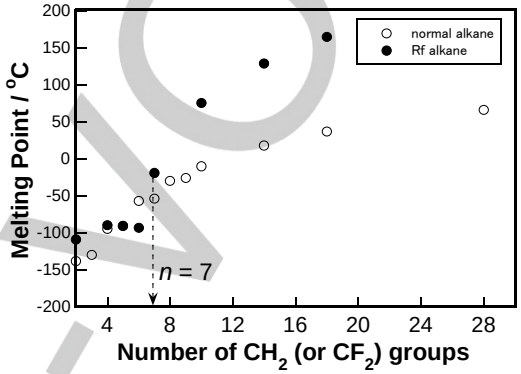

Figure 2. Melting points of normal alkanes (○) and R_f compounds (●) as a function of the chain length. [20,21]

To understand the R_f-specific properties on the chemical structure, the molecular aggregation is considered on the dipole-dipole interaction. Very many dipoles of the C–F bonds located at the helical positions, however, make the discussion unnecessarily complicated. Then, a CF_2 unit is represented by a single dipole moment (see a green vector in Figure 1a) that is a summation of two dipoles of two C–F bonds. Since the R_f-group is a helix, dipoles having different directions at each carbon are available along the R_f-group. If only both ends of the CF_2 chain (the green and pink vectors) are left for simplicity, the *twisting angle of the two vectors reflects the R_f length*.

The twisting rate obeys the phase diagram of PTFE.[5,6,16] At ambient pressure, there are two transition temperatures at T = 19°C and 30°C. The helix has a symmetry of 13_6 and 15_7 for T < 19°C (Phase II) and 19°C < T < 30°C (Phase IV), respectively.[5,6,24-26] For a higher temperature than 30°C (Phase I), the conformation is losing the helicity with temperature.

The symmetry of 13_6 means that the molecule is twisted by 180° over the 12 C–C bonds.[25,27] Therefore, if a compound having $(CF_2)_9$ is considered as illustrated in Figure 1, the pink and green vectors span 120° reflecting the 8 C–C bonds.[27] When the $(CF_2)_9$-containing molecules are packed in a hexagonal manner, the dipoles are interacted in different directions at each carbon (Figure 1b). The *spontaneous 2D aggregation* through the "dipole arrays" is *symbolized by remaining the terminal two vectors only* as found in the top view (Figure 1c). Although only the terminal ends of the $(CF_2)_9$ chain are marked by the two vectors for a better visibility, the rest CF_2 groups also contribute to the 2D spontaneous aggregation (Figure 1b).

This spontaneous hexagonal packing by the dipole-dipole interaction is true of an R_f group having $(CF_2)_9$ or longer (Figure

3c). In other words, $(CF_2)_9$ at shortest is necessary to make the hexagonal packing 'spontaneously.' This molecular aggregation theory considering the 2D dipole arrays network is called Stratified Dipole-Arrays (SDA) theory.[27]

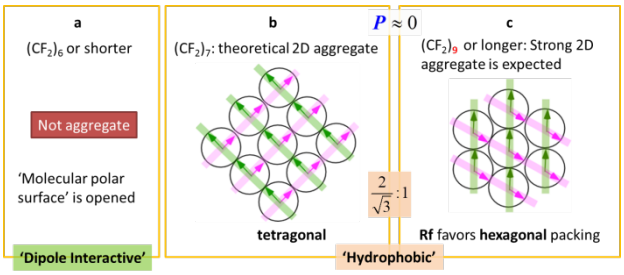

Figure 3. Schematics of the SDA theory depending of the R_f length

This self-aggregation can occur for a little bit shorter length of $(CF_2)_7$ as illustrated in Figure 3b, which is the critical length because the twisting angle (90°) is critically enough to make the molecules aggregated two-dimensionally. As found in the figure, molecules should be in the tetragonal arrangement in the case of $(CF_2)_7$, whose occupying area is larger than the hexagonal one by a factor of $2/\sqrt{3}$, which will be experimentally confirmed in Sect. 2.4. In this manner, *if the twisting angle is 90° or larger*, the dipole arrays are ready for generating a 2D molecular aggregate *exhibiting a bulk character*, which is the criteria on the SDA theory.

If the R_f length is $(CF_2)_6$ or shorter (Figure 3a), the opening of the two dipoles is less than 90°, which is inadequate to make the 2D network via a molecular aggregation.[27] As a result, *a single-molecular character remains* for a short Rf chain, which should attract a molecule having an apparent dipole moment such as "molecular" water (not droplet). This will be discussed later in Sections 2.5 and 2.6. The SDA theory thus enables us to say that $(CF_2)_7$ is the critical minimum length for exhibiting "bulk" characters.

2.3. 'Bulk' Properties on the SDA theory

Once R_f groups are aggregated in accordance with the SDA theory, the melting point should become high because of the tight 2D networks of the dipole arrays, which is definitely not found in the hydrocarbon's case driven by the weak dispersion force.[17] The tight 2D network is difficult to be disaggregated by an approach of a dispersion-driven compound such as chloroform and hexane, which results in a very insoluble character in an organic solvent except Freon-related solvents.[1]

A macroscopic view of the 2D dipole-arrays network accounts for another important property specific to a 'bulk' matter, although the SDA theory is a zeroth-order approximation theory using a simplified image of dipoles. The summation of the dipoles (p ; vectors) involved in the 2D network becomes fairly small (Eq. (5)) because the stratified arrays have different directions (Figure 1b). The summation, P , is called 'polarization density' in electrodynamics.[11]

$$P = \sum p \approx 0 \qquad (5)$$

P is correlated with the electric field, E, via the electric susceptibility, χ_e:[11]

$$P = \varepsilon_0 \chi_e E \,. \qquad (6)$$

ε_0 is a unit-conversion coefficient. On a comparison of Eq. (6) for bulk with Eq. (4) for a single molecule, χ_e can be interpreted as *bulk* polarizability.[3] When this equation is coupled with the next fundamental equation[11] involving the relative electric permittivity, ε_r :

$$\varepsilon_0 \varepsilon_r E = \varepsilon_0 E + P \,, \qquad (7)$$

Eq. (8) is obtained.

$$\varepsilon_r = \chi_e + 1 \qquad (8)$$

This equation straightforwardly implies that "a small permittivity is induced by a small *bulk* polarizability, χ_e ." Note that χ_e cannot be replaced by the molecular polarizability, α , since P depends on the orientation of p , which results in no apparent correlation between χ_e and α .[3]

Eq. (4) is also well known as the fundamental equation of Raman spectroscopy.[28] Raman spectra can be used for discussing molecular polarizability via the Raman tensor analysis, but it cannot be used for discussing permittivity, which needs infrared spectroscopy.[29] This fact supports that the permittivity cannot be discussed by using the molecular polarizability. Then, the question remained is why permittivity is dominated by the bulk polarizability, not by the strong dipole moments composing the 2D dipole-arrays network.

This question is easily solved when we recall that the SDA molecular packing induces an ignorable polarization density, $P \approx 0$ (Eq. (5)). This fact *on a macroscopic view* can be interpreted that a bulk material of an R_f compound has *invisible dipole moments*, although the molecules are aggregated due to the dipoles. As a result, $P \approx 0$ *induces a very low surface energy*, which accounts not only for the water-repellency, but also for the oil-repellency.[1] In addition, $P \approx 0$ also accounts for a small permittivity or a small refractive index ($n = \sqrt{\varepsilon_r}$ [11]) via Eq. (7). In this manner, the SDA theory is a theoretical framework, in which the representative bulk properties of an R_f compound can comprehensively be understood.

The discussion of a bulk property on $P \approx 0$ can also be applied to perfectly random molecules. A representative material having a random orientation is perfluoropolyether (PFPE) represented by $-[CF_2CF_2CF_2\text{-O-}]_n-$. The oxygen atoms in PFPE play a role of flexible joints, which makes the molecule highly flexible as a liquid, although the R_f parts are highly stiff. Since liquid has a character of $P \approx 0$, PFPE also exhibits the water/oil repellency as a bulk property.[30]

2.4. Monolayer study for examining the SDA theory

To examine the SDA theory experimentally, four myristic acid (MA) derivatives are prepared, which have an R_f group with different length at the terminal (Figure 4).

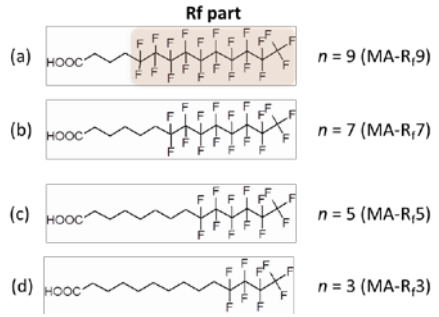

Figure 4. Myristic acids containing a terminal R_f group with different length. Each compound having an R_f group with the length of $(CF_2)_n$ is named "MA-$R_f n$"

On the SDA theory, if a compound having an R_f part with the length of n = 7 or 9 (named as "MA-R_f7" or MA-R_f9) is spread on the water surface, the compounds should be aggregated two-dimensionally to form monolayer domains, in which the molecules should have a perpendicular stance to the water surface (Figure 5a). On the other hand, if a short R_f-containing compound (MA-R_f5 or MA-R_f3) is spread on the water surface, the R_f part would play a role of a dipole-interacting part. As a result, the molecules would lie on the water surface (Figure 5b).

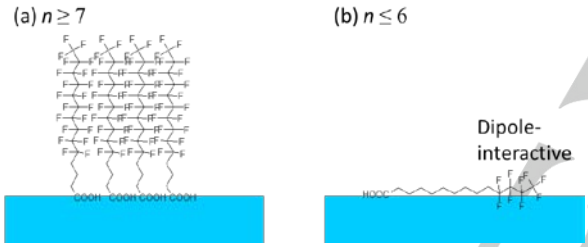

Figure 5. Schematic image of MA-R$_f n$ on the water surface depending on the R_f length. (a) Molecules are spontaneously aggregated two-dimensionally. (b) Molecules would exhibit a single-molecular character.

The surface pressure (π)–surface area (A) isotherms of a Langmuir monolayer of the four compounds on water are presented in Figure 6. For MA-R_f3 and MA-R_f5, a continuous and monotonous increase appears on the monolayer compression. This implies that the molecules are homogeneously spread on water, and they are lying even at an early stage of compression, since π goes up soon after the initial compression at a large surface area.

On the other hand, MA-R_f7 and MA-R_f9 exhibit largely different isotherms: a long nil-line (π = 0) appears before running up at a surface area of ca. 0.4 nm^2 molecule^{-1} or less. This is a typical pattern of a stiff molecular domains generated before the compression as usually found for a spontaneously aggregated monolayer, for example of cadmium stearate.[31]

The linearly increasing part of the stiff monolayers corresponds to the S (solid) phase of the film,[31] and the bottom of the linear part marked by a red circle (at ca. 15 mN m^{-1}) is the position where the molecules are spontaneously aggregated. Therefore, to measure the surface area of the spontaneously aggregated molecules, the surface areas at 15 mN m^{-1} should be taken. As a result, the observed areas of 0.330 and 0.286 nm^2 molecule^{-1} for MA-R_f7 and MA-R_f9, respectively, are beautifully correlated with each other by the factor of $2/\sqrt{3}$, which is predicted by the SDA theory (Figure 3).

$$0.286 \times \frac{2}{\sqrt{3}} = 0.330$$

Through the monolayer study, in this manner, the SDA theory has readily proved to be reasonable. As found in the isotherms, however, the spontaneously achieved the tetragonal packing for MA-R_f7 is kinetically stable, and it is finally changed to the hexagonal one by the further monolayer compression, since the closest packing in terms of crystallinity is preferred on the compression.

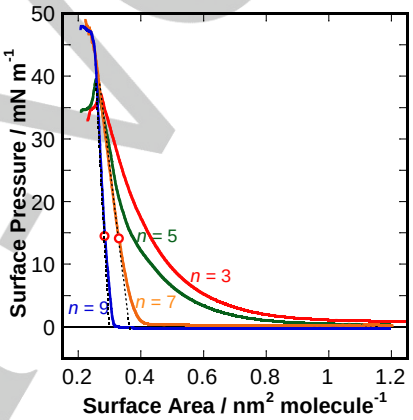

Figure 6. Surface-pressure (π)–surface area (A) isotherms of a monolayer of the compounds in Figure 4. The red circles are at the bottom position of a linear part (solid film), which crresponds to a spontaneously aggregated molecules.

More details of the molecular structure and arrangement in the monolayer will be discussed by using infrared spectroscopy in Sect. 3.

2.5. Property of a 'single molecule' containing an R_f group

The monolayer study in the previous section gives us an impression that the dipole-interacting character of a short R_f group may equal to a "hydrophilic" character. If this interpretation is true, however, the monolayer should partly be dissolved in the subphase water during the monolayer compression. As found in the next paragraph, however, the dipole-interacting character is not an interaction with bulk water, and it should be discriminated from the hydrophilicity.[32]

To discuss the single-molecular character on the water surface, the surface potential (ΔV)–A isotherms as well as the π–A isotherms are measured (Figure 7). ΔV is a measure of a dipole moment in a molecular aggregate, and it thus reflects the molecular density as well as the orientation and hydration changes.[30,32] An MA-R_f5 (or MA-R_f3) molecule has a large dipole moment mostly located at the connecting point between the R_f and the alkyl parts, which is illustrated by an downward arrow in Figure 7. In fact, a negative ΔV appears on compression. The fairly good agreement of the ΔV–A isotherms with the theoretically predicted curve on the molecular density

only (blue dotted curve) implies that MA-R_f5 (or MA-R_f3) molecules are homogeneously spread on water without dissolving in the subphase, and without changing the orientation throughout the compression. The insoluble character means that a short R_f group has a different property from hydrophilic. In addition, keeping the orientation means that a short R_f group has a stable affinity with the water surface, and it is not detached on the compression.

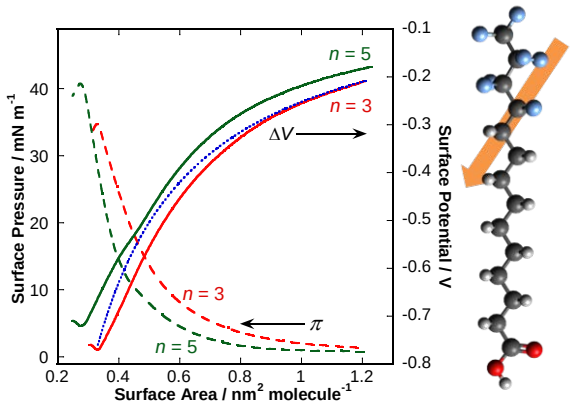

Figure 7. (Left panel) Surface potential (ΔV)–A curves of a monolayer of MA-R_f3 and MA-R_f5. The blue dotted curves are calculated density curves. The π–A curves are simultanesouly obtained with the ΔV–A measurements, but they correspond to those in Figure 6. (Right panel) The arrow is a schamatic of the dipole moment of the molecule.

To understand the high affinity with the water surface in more detail, a comparative study to a normal MA having no R_f group is employed. Simultaneous measurements of π–A and ΔV–A isotherms of normal MA are performed as presented in Figure 8b. The π–A isotherm of MA has the LE (liquid expanded) and LE/LC (liquid condensed) regions, in which the molecular conformation changes accompanying the detachment of the alkyl tail from the water surface, i.e., the *normal alkyl group exhibits a hydrophobic character on the water surface*.[30] This molecular orientation change is not found for an R_f-containing MA (Figure 7). This comparative study indicates that a single molecule of a short R_f-containing MA is stably attached to the water surface throughout the monolayer compression. In other words, *a short R_f group does not exhibit the hydrophobic character, either*, if "hydrophobic" is defined as an exclusive character of water.

In short, a single R_f group is *neither hydrophilic nor hydrophobic*. Instead, the R_f group is stably attached to the water 'surface' because a *single R_f group having a dipole moment at a local C–F bond recognizes hydroxyl groups* available on the water surface.[33] This single R_f group-specific unique character is called "dipole interactive."[32] In this manner, the "scale" of not only R_f group, but also of water is another important key to consider the affinity to water.

The lying stance of a single R_f-containing molecule on the water surface is also confirmed by a detailed analysis of the ΔV-A isotherm (Figure 8b). The rapidly increasing part of ΔV on monolayer compression is correlated with the corresponding π–A curve via "dehydration" about the head group in the water surface.[32] At an early stage of compression, ΔV stays at ca. π = 0 as found for the stearic acid (SA) monolayer (Figure 8a), since the dipole centered about the head group is shielded by the hydration. Therefore, the rapid increase of ΔV indicates a dehydration process removing the hydrated water molecules.

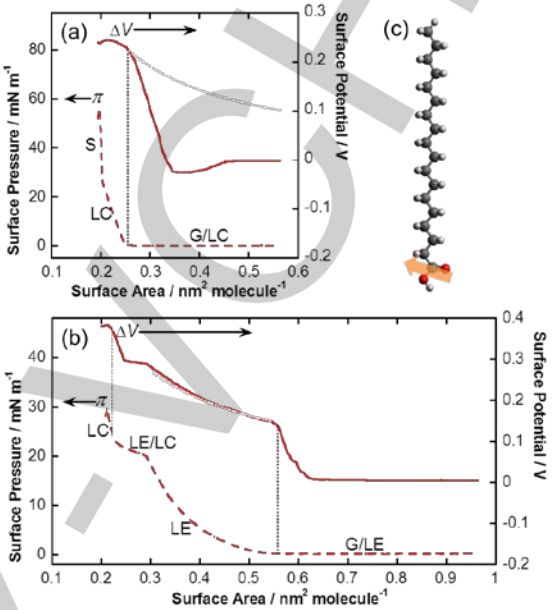

Figure 8. Surface pressure (π; dashed curve) and surface potential (ΔV; solid curve) isotherms of (a) SA and (b) MA having no R_f group against the surface area (A). (c) The dipole moment of the molecule is located near the C=O group with a tilt as presented by the arrow.

When the hydration water is mostly removed by a further monolayer compression, the increase of ΔV stops, and instead the SA molecules are directly interacted with each other to yield a rapid increase of π. This synchronization of π–A and ΔV–A isotherms is commonly found for other compounds as found in Figure 8a and 8b, which is a good marker of dehydration. This schematics about the carboxyl group thus readily explain the nil and positive changes of ΔV.

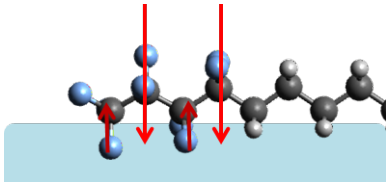

Figure 9. A schematic of a lying molecule in the water surface. A red arrow indicates the dipole moment of a CF_2 group, and the length indicates the intensity after the hydration of the lower-half of the lying molecule.

The isotherms in Figure 7, however, shows an apparently negative ΔV *even before* the monolayer compression. If only the dipole-moment image over the entire molecule (the yellow arrow in Figure 7) is simply taken into account, a negative ΔV can be explained by only the perpendicular molecular stance, and it cannot be explained by the homogeneously spreading molecules with a lying stance (Figure 5b). Fortunately, however, this problem can be solved by considering the dipole moment of each CF_2 group as illustrated in Figure 9. An R_f group attached to the water surface has only the lower-half C–F groups

hydrated, which makes the total C–F bonds have a negative dipole moments irrespective of the rotational orientation about the molecular axis.[32] In this manner, the apparent negative ΔV with a good reproducibility paradoxically supports the lying stance of a single molecule of the short R_f-containing compound on the water surface.

2.6. A disaggregated R_f group adsorbs molecular water

PTFE is a long R_f chain polymer, and the R_f chains in Phase II (below 19°C) are tightly aggregated in a hexagonal manner in most parts exhibiting an extraordinary high melting point at 327°C.[5,34] If a PTFE tape is stretched, for example by 150%, the stretch would make the molecules disaggregated to have a single-molecular character to the air.

This disaggregation phenomenon is often found when we use a PTFE tape in laboratory. Although the surface of the tape has no adhesiveness, a stretched-and-cut PTFE tape sticks to another tape surface, which is useful for sealing a glass bin. This drastic change of the surface property is induced by the appearance of the single molecular character via the molecular disaggregation.

If the molecular disaggregation occurs actually, a single R_f group should attract *molecular* water via the dipole-dipole interaction. Note that a water 'molecule' cannot recognize $P \approx 0$ because of the small size. This prediction is easily confirmed by using ^{1}H NMR: a stretched PTFE tape in ambient air is put in a NMR tube to measure the adsorbed water molecules as presented in Figure 10.[35]

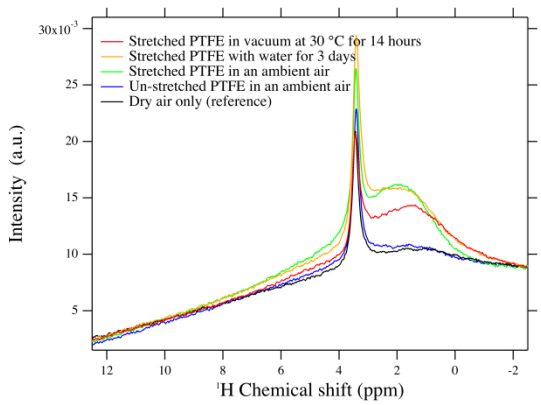

Figure 10. ^{1}H NMR spectra of a (a) unstretched PTFE tape (dark blue), (b) streched one in ambient water (green), (c) stretched one in a saturated water vapor (orange), (d) stretchedone in ambient air followed by evacuation of the NMR tube (red). A reference spectrum of dry air without a tape is presented by the black curve. Ignore the strong sharp peak at 3.4 ppm, which is due to the minute water gas in the temperature-controlling air outside the NMR tube.[35]

Before stretching, the NMR spectrum of a PTFE tape stored in ambient air (dark blue) is nearly the same as that of air only (black), which indicates that an ignorable amount of water exists on the un-stretched PTFE surface. A PTFE tape 1.5-times stretched in length in ambient air, however, exhibits an apparent water peak (green) at about 2.0 ppm. This peak is reproduced by putting a stretched tape in a saturated water vapor (orange), which implies that the polar surface of the disaggregated molecules is fully occupied by adsorbed gaseous water of an ambient air. Once adsorbed on the tape surface, the water molecules are difficult to remove even in a vacuumed condition for 14 hours as presented by the red spectrum.

The position of the water peak after a magnetic susceptibility correction in the sample is 2.1 ppm, which corresponds to the dispersed water molecules in an organic solvent of acetonitrile[36] that has a large dipole moment.[37,38] This is consistent with the expectation on the SDA theory that the water molecules are stuck on an R_f group having a single-molecular character via the dipole-dipole interaction. Thus, the adsorption of molecular water on the stretched PTFE tape is also expected to be strong.

In fact, the water peak has a large peak-width as found in Figure 10, which suggests that the rotation dynamics of the adsorbed water is highly restricted. To discuss the molecular motion quantitatively, 18 spectra were recorded with different mixing time varied from 10 μs to 10 s, and the inversion recovery method[39] was employed to obtain the longitudinal relaxation time, T_1 = 0.557 ± 0.001 sec.[35] This relaxazation time was converted to be the rotation correlation time, τ_c, by solving the theoretical equation (Eq. (9)).[40,41]

$$R_1 = \frac{1}{T_1} = \left(\frac{\mu_0}{4\pi}\right)^2 \left(\frac{3\hbar^2\gamma^4}{10r^6}\right)\left(\frac{\tau_c}{1+\omega_0^2\tau_c^2} + \frac{4\tau_c}{1+4\omega_0^2\tau_c^2}\right) \qquad (9)$$

Here, μ_0 is the magnetic permeability in vacuum, γ is the gyromagnetic ratio of proton, r is the distance between two protons in a water molecule, and ω_0 is the Larmor frequency. As a result, τ_c is obtained to be 44 ns, which is much longer than that of neat water, 2.6 ps,[42] and comparable to the first and second hydration water about the sulfonate group exhibiting 8.8 and 220 ns, respectively.[43] In this manner, the adsorbed molecular water on a stretched PTFE tape is revealed to be highly restricted in rotational motion.

It is of another note that the contact angle was ca. 123° for both un-stretched and stretched tapes.[35] Since the contact angle measurements were performed by using a water "droplet" with a volume of 4 μL, which is a bulky scale, a water droplet feels $P \approx 0$ irrespective of the stretch via a 2D macroscopic averaging.

3. Vibrational spectroscopy for R_f-containing compounds

Molecular vibration is another important material property, and the vibration of an R_f group is significantly different from that of a normal alkyl group. This straightforwardly influences infrared (IR) and Raman spectroscopy greatly, and the conventional common sense of a normal alkyl group cannot be employed.

3.1. Concept of "group vibration" greatly changes

The fundamental of molecular vibration is the normal mode,[29] which is the natural vibration of a molecule, and in general the vibration can be regarded as a localized vibration at a specific

chemical group. Therefore, the normal mode is often interpreted as the "group vibration," which is conveniently used for chemical analysis. Note, however, that this concept is true of normal hydrocarbon.

Another crucial difference between the normal alkyl and R_f groups is the relative mass of hydrogen and fluorine to carbon, respectively. Since the mass of hydrogen is smaller than that of carbon ($m_H < m_C$), only hydrogen atoms seem to vibrate while carbon atoms stay unmoved for a normal alkyl group. In the case of an R_f group, on the other hand, the mass of fluorine is larger than that of carbon ($m_F > m_C$). Therefore, the fluorine atoms relatively stay unmoved, and instead *the carbon atoms are vibrated*. Since the carbon atoms are directly connected, the vibration cannot be localized at a specific chemical group, but it is spread over the R_f group as illustrated in Figure 11b.

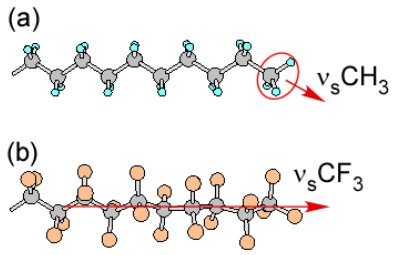

Figure 11. Schematic image of a normal mode of (a) ν_sCH_3 and (b) ν_sCF_3. A red arrow indicates the direction of the transition moment.

For example, let us consider the symmetric CH_3 stretching vibration (ν_sCH_3) mode. Very strictly speaking, the vibration of this mode is spread over the molecule, but it can be regarded as a local vibration only on the terminal methyl group (red circle) within a good approximation. Therefore, the direction of the transition moment of the ν_sCH_3 mode can be represented by the red arrow in Figure 11a. On the other hand, the symmetric CF_3 stretching vibration (ν_sCF_3) mode has the direction of the transition moment nearly along the R_f group (Figure 11b).[44] This will be used for molecular orientation analysis of the R_f group as discussed later for Figure 13.

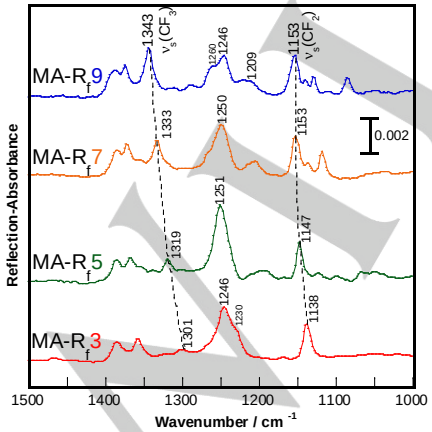

Figure 12. IR RA spectra of a monolayer LB film of MA-R$_f$*n* deposited on a gold surface transferred at 15 mN m^{-1}. Both ν_sCF_3 and ν_sCF_2 bands are shifted on the R_f length as indicated by the dashed lines.

Figure 12 presents IR reflection-absorption (RA) spectra[29,45,46] of a single monolayer Langmuir-Blodgett (LB) film of MA-R$_f$*n* deposited on gold at the surface pressure of 15 mN m^{-1}, at which the monolayer is fully covered with spontaneously aggregated molecules (see Figure 6). The band at 1153 cm^{-1} of MA-R$_f$9 is assigned to the symmetric CF_2 stretching vibration (ν_sCF_2) band. This assignment is a temporal one, which needs more complicated duscussion based on a factor group analysis[5] considering the phase difference between the adjacent CF_2 units along the coupled oscillattor.[6] Regardless, the assignment is quite useful with no severe problem for many practical purposes. The band at 1246 cm^{-1} is often roughly assigned to the anti-symmetric CF_2 stretching vibration (ν_aCF_2) band, but it still has an argued problem.[44]

Of note is that the ν_sCF_3 mode is located at 1343 cm^{-1}. Since this position is higher than the ν_aCF_2 position, it seems extraordinarily high in the sense of a normal hydrocarbon. The reason is, however, simple that the ν_sCF_3 mode is spread over the R_f group, and the wavenumber reflects the coupled oscillation of the entire R_f group. In fact, the band position of this mode is largely shifted depending on the R_f length as found in Figure 12. A similar shift is also found for the ν_sCF_2 band.

All the MA-R$_f$*n* compounds commonly have 'one' CF_3 group at the terminal, but the intensity of the ν_sCF_3 band varies a lot: the intensity is very strong for MA-R$_f$9 while it is largely suppressed for MA-R$_f$3. Judging from the "surface selection rule" of RA spectrometry that only the surface-perpendicular component of a normal mode appears in the spectra, the difference of the band intensity tells us that MA-R$_f$9 stands perpendicularly; whereas MA-R$_f$3 lies on the surface because of the direction of the transition moment (Figure 11b). This molecular scheme agrees with the schematic images in Figure 5 discussed on the π–*A* isotherms in Figure 6.

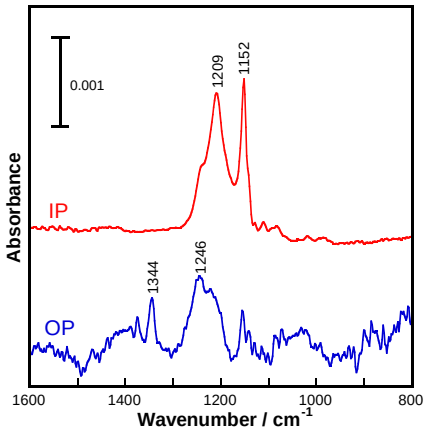

Figure 13. IR pMAIRS spectra of a single monolayer LB film of MA-R$_f$9 deposited on a silicon substrate transferred at a surface pressure of 15 mN m^{-1}.

Since the RA spectrometry detects only the surface perpendicular component, however, it is difficult to conclude the R_f group of MA-R$_f$9 has a 'perfectly' perpendicular stance to the surafce. The pMAIRS technique[47-51] works powerfully for this purpose, since it provides both in-plane (IP) and out-of-plane (OP) spectra from an identical thin-film sample. The IP and OP

spectra corresponds to the conventional transmission and RA spectra, respectively.[29]

Figure 13 presents IR pMAIRS spectra[44] of a single-monolayer LB film of MA-R_f9 deposited on a silicon substrate at the same surface pressure of 15 mN m^{-1} as that for the RA spectra in Figure 12. The OP spectrum corresponds to the RA spectrum of the MA-R_f9 monolayer (top of Figure 12). The vibration of the normal hydrocarbon part travels through the R_f part, which makes the OP spectrum highly complicated.[44] On the other hand, the IP spectrum is nearly free from the influence of the normal hydrocarbon part, and the IP spectrum becomes much simpler.

In the pMAIRS spectra, note that the $\nu_s CF_3$ band (1344 cm^{-1}) appears only in the OP spectrum, and no band is available in the IP one. Since the transition moment of this mode is along the R_f group, this result straightforwardly implies that the R_f group is perpendicularly oriented to the film surface with almost no tilting.

The reader may consider that the orientation analysis can also be performed by using the symmetric "CF_2" stretching vibration ($\nu_s CF_2$) mode as is often used for analysis of a normal alkyl group. As a matter of fact, however, this is another R_f-specific notable point, which is largely different from a normal alkyl group. Since an R_f group has a helical conformation, a tilted R_f group has a parallel $\nu_s CF_2$ mode as well as a tilted one depending on the carbon position of the R_f group. Therefore, the $\nu_s CF_2$ band *cannot* be used for molecular orientation analysis.[27]

3.2. Berreman effect is necessary for analysing R_f group

One of the selection rules of IR spectroscopy is formulated by Eq. (10).[29,45]

$$\left(\frac{\mathrm{d}\mu}{\mathrm{d}x}\right)_0 \neq 0 \qquad (10)$$

Here, μ is the dipole moment involving both permanent and induced components, and x is the length of the dipole. This equation means that the IR absorption becomes stronger for a dipole having a larger permanent dipole moment. Since the C–F bond has an extremely large permanent dipole moment (cf. Table 1), IR bands relevant to a C–F stretching vibration exhibit farily large intensities.

As a matter of fact, an IR absorption spectrum of a *condensed matter* reflects the electric permittivity, not a dipole moment directly.[29] The permittivity is described by using the relative permittivity, ε_r, as defined by Eq. (7).[11,29] When the spectrum consists of multiple-number of bands, the permittivity function, $\varepsilon_r(\omega)$, is theorized by Eq. (11).[11,29,45]

$$\varepsilon_r(\omega) = \varepsilon_{r,\infty} + \omega_p^2 \sum_j \frac{f_j}{\omega_j^2 - \omega^2 - \mathrm{i}\gamma_j\omega} \qquad (11)$$

Here, $\varepsilon_{r,\infty}$ and ω_p are permittivity at a high frequency and the plasma frequency, respectively. The rest parameters of f_j and γ_j are the oscillator strength (corresponding to the band intensity) and the damping factor (corresponding to the band width) of a band at ω_j, respectively.

With the use of the permittivity, transmission and RA spectra (corresponding to pMAIRS–IP and –OP spectra, respectively) are physically described as a solution of Maxwell equations considering an optical interface as follows.[29,45]

$$A^{\mathrm{Tr}}{}_{\theta_1=0} = \frac{1}{\ln 10\cdot\lambda}\cdot\frac{8\pi d_2}{n_1+n_3}\mathrm{Im}\left(\varepsilon_{\mathrm{r}\,x,2}\right) \qquad (12)$$

$$A^{\mathrm{RA}} = \frac{8\pi d_2}{\ln 10\cdot\lambda} n_1{}^3 \frac{\sin^2\theta_1}{\cos\theta_1}\mathrm{Im}\left(-\frac{1}{\varepsilon_{\mathrm{r}\,z,2}}\right) \qquad (13)$$

The parameters of n_m and $\varepsilon_{\mathrm{r}\,x,m}$ are the refractive index and the relative permittivity of the m^{th} phase, and θ_1 is the angle of incidence. The air, film and substrate phases are indexed by 1, 2 and 3, respectively, and d_2 is the film thickness. *x* and *z* mean the surface parallel and perpendicular, respectively. The spectra-shape of the transmission and RA spectra is dominated by the functions of $\mathrm{Im}(\varepsilon_r)$ and $\mathrm{Im}(-1/\varepsilon_r)$, respectively, which are called TO and LO energy-loss functions.[29,45]

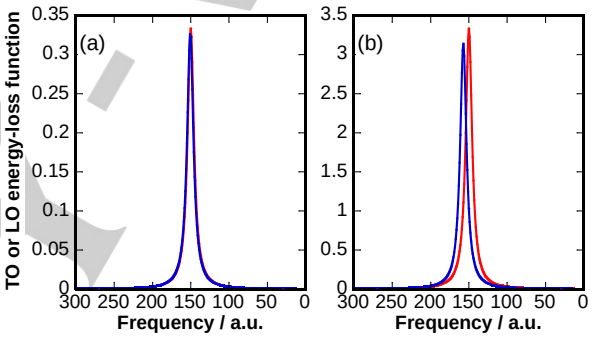

Figure 14. Simulated TO (red) and LO (blue) energy-loss function spectra calculated by using Eq. (11) with the electric permittivity on $\varepsilon_{r,\infty}=2.25$, $\omega_0=150$, $\gamma=10$ for a weak absorber ($\omega_p{}^2 f=500$) and (b) a strong absorber ($\omega_p{}^2 f=5000$).

For a weak IR absorbing material such as a normal hydrocarbon, the TO and LO functions appear at nearly the same position as presented in Figure 14a.[29] This means that we don't have to take care about the difference of the measurement techniques for a normal alkyl group.

For a strong IR absorbing material, on the other hand, the LO peak appears at an apparently higher-shifted position than the TO peak (Figure 14b). This band shift due to the strong absorption is called "Berreman effect."[29,52] In other words, a strongly absorbing band would appear at different positions depending on the measurement techniques, which makes the discussion confusing, and sometimes lead us to a wrong direction. Therefore, we have to convert the measured spectra to a specific function, for example, LO function spectra.

Here, an example of spectral conversion is presented through a practical monolayer analysis. To discuss the molecular orientation and packing, the RA spectra of monolayers in Figure 12 should be compared to spectra of bulk (un-oriented) samples. The bulk spectra are conveniently obtained by using the ATR technique.[29,44] Figure 15 presents IR ATR 'raw' spectra of bulk materials of the MA-R_f*n* series before conversion.

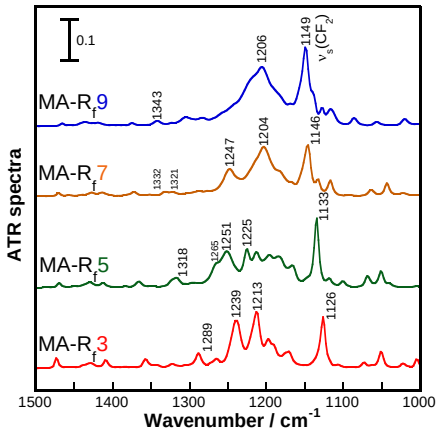

Figure 15. IR ATR "raw" spectra of bulk materials of MA-R$_f$*n* before spectral conversion

When the ATR spectrum of MA-R$_f$9 is compared with the corresponding RA spectrum in Figure 12, for example, we find that the $\nu_s CF_2$ mode appears at different positions of 1153 and 1149 cm^{-1}, respectively. At this stage, the difference of band position *cannot be attributed to a difference of chemical structure* between the monolayer and the bulk matter, since it may be induced by the Berreman effect.

An ATR spectrum is a linear combination of TO and LO spectra,[29,45] and thus the spectrum cannot directly be compared with an RA spectrum of a strong IR absorber especially for the band position, which needs a spectral conversion. Fortunately, ATR spectra can be converted to complex electric permittivity, $\varepsilon_r(\omega)$, by using Kramers-Kronig (KK) relations.[29,45,53] Note that the refractive index of the material, n, is needed for putting $\varepsilon_{r,\infty}(=n^2)$ as found in Eq. (11). For most organic materials, $n=1.55$ can conveniently be used, but $n=1.35$ is recommended for R$_f$ compounds.[52,54] Once $\varepsilon_r(\omega)$ is calculated, the TO and LO function spectra are readily obtained through Eqs. (12) and (13).

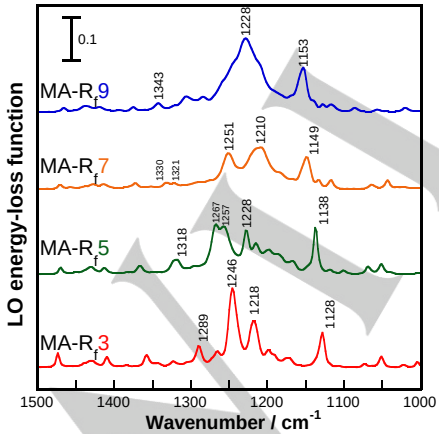

Figure 16. The LO energy-loss function spectra of bulk materials converted from the ATR spectra in Figure 15. These converted spectra are ready for comparison with the RA spectra in Figure 12.

The LO energy-loss function spectra converted from the ATR spectra in Figure 15 are presented in Figure 16. The LO spectrum of MA-R$_f$9 exhibits the $\nu_s CF_2$ band at 1153 cm^{-1}, which beautifully agrees with the corresponding RA spectrum.[27] In this manner, an R$_f$-containing compound often yields Berreman's shift, which must be removed from the chemical discussion by an appropriate conversion using KK relations.

The $\nu_s CF_2$ position is useful for discussing the molecular packing. With the converted LO spectra of the bulk matters, we are ready for discussing the molecular packing in the monolayer. The comparison with the RA spectra of the monolayers is summarized in Table 2.

Table 2. Comparison of the band positions of the bulk matter and the monolayer via the ATR-LO and RA spectra, respectively.

n	$\nu_s(CF_2)$ / cm^{-1}		Δ / cm^{-1}
	bulk (ATR-**LO**)	monolayer (RA)	
9	1153	1153	0
7	1149	1153	4
5	1138	1147	9
3	1128	1138	10

The agreement of the position for MA-R$_f$9 implies that the *spontaneously aggregated molecular packing* at 15 mN m^{-1} in the monolayer *is the same as that in the bulk matter*. This strongly supports the SDA prediction that an R$_f$ group having $(CF_2)_9$ or longer would tightly be aggregated two dimensionally. In a similar manner, the large higher-wavenumber shift found especially for MA-R$_f$3 and MA-R$_f$5 indicates that a short R$_f$ chain-containing molecules cannot be aggregated spontaneously, since the molecules are lying on the water surface stably through the monolayer compression as discussed in Sect. 2.5.

In this manner, the monolayer studies in former sections have rigidly been confirmed by accurate and quantitaive IR spectroscopy considering some R$_f$-specific spectroscopic characters.

4. Phase transition

The experimental studies in the previous sections were all performed at the temperature of 15 °C (Phase II), in which the R$_f$ group has the helical conformation of 13_6.[5,6,24-26] On referring to the phase diagram at ambient pressure, the conformation would be changed to be 15_7 at 25 °C (Phase IV). The conformational change is interpreted as a decrease of the twisting angle of the two CF_2 dipole at both ends of the R$_f$ group as schematically illustrated in Figure 17.

As mentioned in Sect. 2.2, the critical angle for the spontaneous 2D aggregation is 90°. In Phase II, an R$_f$ length of $(CF_2)_7$ (i.e., n = 7) or longer satisfies this condition. When the temperature goes up across 19°C, n = 9 or longer satisfies this condition, but n = 7 is too short as well as n = 5 or less. This means that when a bulk measurements such as ΔV–A isotherms are performed at a temperature above 19°C, only the results of n = 7 would drastically be changed; whereas the rest samples would exhibit ignorable change on the temperature change.

In fact, when the ΔV–A and π–A isotherms were measured at 25°C, only the curves of n = 7 were selectively

changed leaving the rest curves unchanged.[32] This agreement with the theoretical prediction suggests that the SDA theory is powerful for comprehensive understanding of R_f-containing compounds.

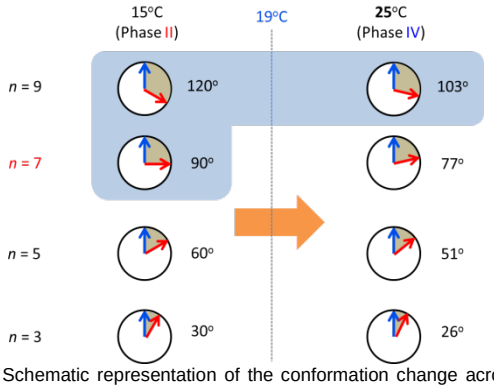

Figure 17. Schematic representation of the conformation change across the transition temperature of 19 °C. The twisting rate depending on the R_f length is represented by the angle spanned by the blue and red arrows.

5. Conclusion

Key concepts for comprehensive understanding of R_f-containging compounds are summarized as: 1) a single molecule exhibits a totally different properties from a bulk matter, 2) R_f groups prefer hexagonal molecular packing induced by the dipole-dipole interaction and the R_f-specific helical conformation, 3) 2D dipole arrays network yields $P \approx 0$, which produces both water and oil repellencies, which has temporarily been attributed to the fluorous effect. On considring that the helical conformation is induced by the steric repulsion between fluorine atoms having a larger radii than hydrogen, most of the “unique” characters of R_f-containing compounds are attributed to only the two characters of fluorine: the large electronegativity and the large radii. If the relatively larger mass of fluorine than hydrogen is taken into account, the unique R_f-specific vibrational spectroscopy can also be understood. This technical improvement is of course applicable to a wide range of monolayer analysis, in which the molecular orienataion is a key to understand the material function.[55-57]

As an application on this theoretical concept, for example the proton transport across a Nafion® membrane is readily understood. The R_f chains of Nafion ‘having many branches’ inhibits the molecular aggregation, which results in generating a single-molecular character here and there. As found in the study of a stretched PTFE tape, the branched-R_f block in the membrane should be hydrophobic for bulky water; whereas it should thus have high affinity to molecular water, which transports proton with an aid of hopping ports of the sulfonic acid group.

Keywords: Perfluoroalkyl compound, material property, stratified dipole-arrays theory, dipole interactive, infrared spectroscopy

1 M. P. Krafft, J. G. Riess, *Chem. Rev*. **2009**, *109*, 1714–1792.
2 C. R. Martinez, B. L. Iverson,*Chem. Sci.* **2012**, *3*, 2191–2201.
3 T. Hasegawa, *Chem. Phys. Lett*. **2015**, *627*, 64–66.
4 T. Shimanouchi, *J. Phys. Chem. Refer. Data* **1972**. p. 222.
5 L. Piseri, B. M. Powell, G. Dolling, *J. Chem. Phys*. **1973**, *58*, 158–171.
6 J. F. Rabolt, B. Fanconi, *Macromolecules* **1978**, *11*, 740–745.
7 I. T. Horváth, *Acc. Chem. Res.* **1998**, *31*, 641–650.
8 J. N. Israelachvili in *Intermolecular and Surface Forces*, *2nd Ed.*, Academic Press, London, **1991**, pp. 83–136.
9 P. Atkins, J. de Paula in *Physical Chemistry*, *8th Ed.*, Oxford University Press, Oxford, **2006**, pp. 629–651.
10 F. London, *Trans. Faraday Soc.* **1937**, *33*, 8–26.
11 J. D. Jackson in *Classical electrodynamics 3rd Ed*. Wiley, Hoboken, **1999**.
12 A. D. McLachlan, *Proc. R. Soc. Lond. Ser. A* **1963**, *202*, 224–243.
13 C. W. Bunn, E. R. Howells, *Nature* **1954**, *174*, 549–551.
14 K. Ute, R. Kinoshita, K. Matsui, N. Miyatake, K. Hatada, *Chem. Lett*. **1992**, *21*, 1337–1340.
15 K. Monde, N. Miura, M. Hashimoto, T. Taniguchi, T. Inabe, *J. Am. Chem. Soc*. **2006**, *128*, 6000–6001.
16 S. Hirakawa, T. Takemura, *Jpn. J. Appl. Phys*. **1969**, *8*, 635–641.
17 F. Khoury, B. Fanconi, J. Barnes, L. Bolz, *J. Chem. Phys.* **1973**, *59*, 5849–5857.
18 K. Larsson, *J. Am. Oil Chem. Soc*. **1966**, *43*, 559–562.
19 W. E. Garner, F. C. Randall, *J. Chem. Soc.* **1924**, *124*, 881–896.
20 C. W. Bunn, *J. Polym. Sci. B* **1996**, *34*, 799–819.
21 H. W. Starkweather, *Macromol*. **1986**, *19*, 1131–1134.
22 K. Honda, M. Morita, H. Otsuka, A. Takahara, *Macromol.* **2005**, *38*, 5699–5705.
23 M. Matsunaga, T. Suzuki, K. Yamamoto, T. Hasegawa, *Macromol*. **2008**, *41*, 5780–5784.
24 J. F. Rabolt, B. Fanconi, *Polymer* **1977**, *18*, 1258–1264.
25 H. Flack, *J. Polym. Sci. Part 2 Polym. Phys.* **1972**, *10*, 1799–1809.
26 E. S. Clark, *Polymer* **1999**, *40*, 4659–4665.
27 T. Hasegawa, T. Shimoaka, N. Shioya, K. Morita, M. Sonoyama, T. Takagi, T. Kanamori, *ChemPlusChem* **2014**, *79*, 1421–1425 .
28 Y. Itoh, T. Hasegawa, *J. Phys. Chem. A* **2012**,*116*, 5560–5570.
29 T. Hasegawa in *Quantitative Infrared Spectroscopy for Understanding of a Condensed Matter*, Springer, Tokyo, **2017**.
30 T. Trombetta, P. Iengo, S. Turri, *J. Appl. Polym. Sci.* **2005**, *98*, 1364–1372.
31 G. L. Gains, Jr. *Insoluble monolayers at liquid-gas interface*, Wiley, New York, **1966**.
32 T. Shimoaka, Y. Tanaka, N. Shioya, K. Morita, M. Sonoyama, H. Amii, T. Takagi, T. Kanamori, T. Hasegawa, *J. Colloid Interf. Sci.* **2016**, *483*, 353–359.
33 O. Björneholm, M. Hansen, A. Hodgson, L.-M. Liu, D. Limmer, A. Michaelides, P. Pedevilla, J. Rossmeisl, H. Shen, G. Tocci, et al.,*Chem. Rev.* **2016**, *116*, 7698–7726.
34 C. A. Sperati, H. W. Starkweather, Jr, *Fortschr. Hochpolym. - Forsch.* **1961**, *2*, 465–495.
35 C. Wakai, T. Shimoaka, T. Hasegawa, *J. Phys. Chem. B* **2016**, *120*, 2538–2543.
36 M. Nakakaha, C. Wakai, *Chem. Lett*. **1992**, 809-812.
37 P. A. Steiner, W. Gordy, *J. Mol. Spectrosc*. **1966**, *21*, 291–301.
38 C. Desfrançois, H. Abdoul-Carime, C. Adjouri, N. Khelifa, J. P. Schermann, *Eur. Lett*. **1994**, *26*, 25–30.
39 H. Y. Carr, E. M. Purcell, *Phys. Rev.* **1954**, *94*, 630–638.
40 C. Wakai, T. Shimoaka, T. Hasegawa, *Anal. Chem*. **2013**, *85*, 7581–7587.
41 N. Bloembergen, E. Purcell, R. Pound, *Phys. Rev.* **1948**, *73*, 679–712.
42 D. Lankhorst, J. Schriever, J. C. Leyte, *Phys. Chem*. **1982**, *86*, 215–221.
43 T. Shimoaka, C. Wakai, T. Sakabe, S. Yamazaki, T. Hasegawa, *Phys. Chem. Chem. Phys.* **2015**, *17*, 8843–8849.

44 T. Hasegawa, T. Shimoaka, Y. Tanaka, N. Shioya, K. Morita, M. Sonoyama, H. Amii, T. Takagi, T. Kanamori, *Chem. Lett.* **2015**, *44*, 834–836.
45 V. P. Tolstoy, I. V. Chernyshova, V. A. Skryshevsky in *Handbook of Infrared Spectroscopy of Ultrathin Films*, Wiley, Chichester, **2003**.
46 M. Tasumi (ed.) in *Introduction to Experimental Infrared Spectroscopy: Fundamentals and Practical Methods*, Wiley, Chichester, **2014**.
47 T. Hasegawa, *J. Phys. Chem. B* **2002**, *106*, 4112–4115.
48 T. Hasegawa, *Anal. Chem.* **2007**, *79*, 4385–4389.
49 T. Hasegawa, *Appl. Spectrosc. Rev.* **2008**, *43*, 181–201.
50 N. Shioya, T. Shimoaka, K. Eda, T. Hasegawa, *Phys. Chem. Chem. Phys.* **2015**, *17*, 13472–13479.
51 M. Hada, N. Shioya, T. Shimoaka, K. Eda, M. Hada, T. Hasegawa, *Chem. Eur. J*. **2016**, *22*, 16539–16546.
52 N. Shioya, T. Shimoaka, R. Murdey, T. Hasegawa, *Appl. Spectrosc.* **2017**, in press. (DOI: 10.1177/0003702816676492)
53 J. S. Plaskett, P. N. Schatz, *J. Chem. Phys.* **1963**, *38*, 612–617.
54 N. Shioya, S. Norimoto, N. Izumi, M. Hada, T. Shimoaka, T. Hasegawa, *Appl. Spectrosc.* **2017**, *71*, 901-910.
55 M. Miah, M. Shahabuddin, M. Karikomi, M. Salim, E. Nasuno, N. Kato, K. Iimura, *Bull. Chem. Soc. Jpn.* **2016**,*89*, 203–211.
56 T. Konishi, T. Hashimoto, N. Sato, K. Nakajima, K. Yamaguchi, *Bull. Chem. Soc. Jpn.* **2016**, *89*, 125–134.
57 D. Ishikawa, T. Mori, Y. Yonamine, W. Nakanishi, D. Cheung, J. Hill, K. Ariga, *Angew. Chem. Int. Ed.* **2015**, *54*, 8988–8991.

Entry for the Table of Contents

PERSONAL ACCOUNT

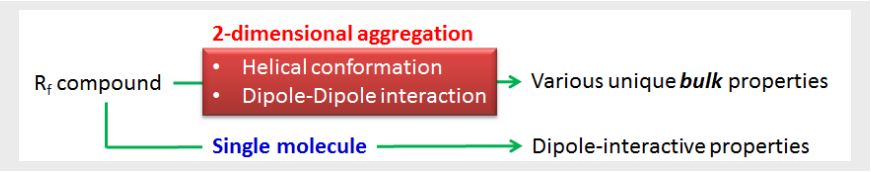

*Takeshi Hasegawa**

Page No. – Page No.

Physicochemical Nature of Perfluoroalkyl Compounds Induced by Fluorine

Perfluoroalkyl (R_f) compounds exhibit unique bulk properties, which cannot be explained by an extended or corrected concept of normal alkyl compounds depending on the dispersion force. The helical conformation of an R_f group induces two-dimensional tight molecular aggregation generated cooperatively with the dipole-dipole interaction, which results in invisible dipoles in a bulk scale accounting for the R_f-specific properties comprehensively.